

Lawrence Berkeley National Laboratory

LBL Publications

Title

Carbon cycle confidence and uncertainty: Exploring variation among soil biogeochemical models

Permalink

<https://escholarship.org/uc/item/79d8n030>

Journal

Global Change Biology, 24(4)

ISSN

1354-1013

Authors

Wieder, William R
Hartman, Melannie D
Sulman, Benjamin N
et al.

Publication Date

2018-04-01

DOI

10.1111/gcb.13979

Peer reviewed

Carbon cycle confidence and uncertainty: Exploring variation among soil biogeochemical models

William R. Wieder^{1,2} | Melannie D. Hartman^{2,3} | Benjamin N. Sulman⁴ | Ying-Ping Wang^{5,6} | Charles D. Koven⁷ | Gordon B. Bonan²

¹ Institute of Arctic and Alpine Research, University of Colorado, Boulder, CO, USA ² Climate and Global Dynamics Laboratory, National Center for Atmospheric Research, Boulder, CO, USA ³ Natural Resource Ecology Laboratory, Colorado State University, Fort Collins, CO, USA ⁴ Program in Atmospheric and Oceanic Sciences, Princeton University, Princeton, NJ, USA ⁵ South China Botanical Garden, Chinese Academy of Sciences, Guangzhou, China ⁶ CSIRO Oceans and Atmosphere, Aspendale, Vic., Australia ⁷ Climate and Ecosystem Sciences Division, Lawrence Berkeley National Laboratory, Berkeley, CA, USA

Correspondence William R. Wieder, Institute of Arctic and Alpine Research, University of Colorado, Boulder, CO, USA. Email: wwieder@ucar.edu

Abstract

Emerging insights into factors responsible for soil organic matter stabilization and decomposition are being applied in a variety of contexts, but new tools are needed to facilitate the understanding, evaluation, and improvement of soil biogeochemical theory and models at regional to global scales. To isolate the effects of model structural uncertainty on the global distribution of soil carbon stocks and turnover times we developed a soil biogeochemical testbed that forces three different soil models with consistent climate and plant productivity inputs. The models tested here include a first-order, microbial implicit approach (CASA-CNP), and two recently developed microbially explicit models that can be run at global scales (MIMICS and CORPSE). When forced with common environmental drivers, the soil models generated similar estimates of initial soil carbon stocks (roughly 1,400 Pg C globally, 0–100 cm), but each model shows a different functional relationship between mean annual temperature and inferred turnover times.

Subsequently, the models made divergent projections about the fate of these soil carbon stocks over the 20th century, with models either gaining or losing over 20 Pg C globally between 1901 and 2010. Single-forcing experiments with changed inputs, temperature, and moisture suggest that uncertainty associated with freeze-thaw processes as well as soil textural effects on soil carbon stabilization were larger than direct temperature uncertainties among models. Finally, the models generated distinct projections about the timing and magnitude of seasonal heterotrophic respiration rates, again reflecting structural uncertainties that were related to environmental sensitivities and assumptions about physicochemical stabilization of soil organic matter. By providing a computationally tractable and numerically consistent framework to evaluate models we aim to better

understand uncertainties among models and generate insights about factors regulating the turnover of soil organic matter.

1 INTRODUCTION

Soils represent the largest terrestrial carbon pool on Earth, storing nearly five times as much carbon as vegetation (Jobbágy & Jackson, 2000). In the new millennium, the theoretical understanding of factors responsible for soil organic matter stabilization has undergone significant revisions (Lehmann & Kleber, 2015; Schmidt et al., 2011). Driven by new measurements that afford high resolution information on the chemical and physical nature of soil organic matter, these emerging theories posit that microbial access to otherwise decomposable substrates (as opposed to inherent chemical recalcitrance) governs soil organic matter stabilization and turnover. Such insights, however, remain poorly represented in global-scale models that investigate potential carbon cycle – climate feedbacks (Luo et al., 2016; Wieder, Allison, et al. 2015), despite an expansion in the number and diversity of soil biogeochemical models (Manzoni & Porporato, 2009; Sierra, Müller, & Trumbore, 2012). Building the capacity to test emerging ecological theories in global-scale models is critical to informing future research needs, testing soil biogeochemical theory, refining model features, and accelerating advancements across scientific disciplines.

Earth system models (ESMs) are typically applied to project potential carbon cycle – climate interactions and inform policy decisions (Ciais et al., 2013), but these models also represent a scientific tool to test ecological insight at larger spatial and longer temporal scales. In global-scale applications where ESMs are used to generate numerical projections, soil biogeochemical models show large variation in estimates of present day soil carbon storage and widely divergent projections of soil carbon response to environmental change (Tian et al., 2015; Todd-Brown et al., 2013). When propagated into future scenarios, this creates uncertainties in the magnitude of terrestrial carbon uptake (Anav et al., 2013; Arora et al., 2013; Friedlingstein et al., 2014; Hoffman et al., 2014), and presents limitations for assessing the allowable carbon emissions that are compatible with desired climate outcomes (Jones et al., 2013, 2016; Zhang, Wang, Mearns, Pitman, & Dai, 2014). Troublingly, the soil biogeochemical models of these studies share a common structure, and thus fail to incorporate process uncertainties associated with factors regulating soil organic matter stabilization in soils. As such, they potentially underestimate the true uncertainty associated with soil carbon responses to environmental perturbations (Bradford, Wieder, et al., 2016). Moreover, without applying these emerging soil biogeochemical concepts into global scale models, opportunities to deepen ecological insight by evaluating and refining theories are not being fully realized.

Building confidence in terrestrial carbon cycle projections, therefore, requires consideration of the factors controlling the decomposition and formation of soil organic matter (Bradford, Wieder, et al., 2016). This research priority

requires balancing demands between formulating model structures that adequately represent theoretical understanding of processes relevant for long-term soil organic matter dynamics and avoiding undue complexity (Luo et al., 2016; Wieder, Allison, et al. 2015). More practically, it requires a numerically consistent, computationally efficient simulation framework that can be used to compare and evaluate models at ecosystem- to global scales. Overlying terrestrial models generate additional variation in the biogeochemical and biophysical state upstream of the soil system—including uncertainties in climate, hydrology, and plant productivity – and the potential ecosystem responses of these factors to perturbations (Todd-Brown et al., 2013, 2014). Although such considerations are critical for assessing the integrated terrestrial carbon cycle response to environmental change, they present unnecessary impediments to assessing the soil biogeochemical component of terrestrial models and advancing understanding of soil systems. Moreover, as soils respond slowly to perturbations relative to many of these upstream factors, modifications of soil model structures and parameterizations often extend spin-up time, which ultimately slows model development (Exbrayat, Pitman, & Abramowitz, 2014; Koven, Chambers, et al., 2015). To address these challenges, we developed a soil biogeochemical testbed that facilitates the evaluation of and improvements to the process-level representation of global-scale soil biogeochemical models.

We compare three soil biogeochemical models that make distinct assumptions about the processes and factors regulating the formation and decomposition of soil organic matter. One of the models reflects traditional ideas about the inherent chemical recalcitrance of soil organic matter. Thus, it implicitly represents microbial activity and follows a conventional decomposition cascade regulated by first-order decay kinetics (Bradford & Fierer, 2012; Schimel, 2001). The other two models explicitly represent soil microbial activity and physiology, but make different assumptions about interactions between microbial community activity and the physicochemical soil environment. Recognizing that multiple sources of uncertainty generate spread among models, in this paper we focus on quantifying model structural uncertainty by comparing steady state soil carbon stocks, turnover times, and their responses over a transient simulation with soil biogeochemical models that are forced with identical inputs and environmental conditions.

2 MATERIALS AND METHODS

We created the biogeochemical testbed to conduct global-scale soil biogeochemistry simulations using a variety of forcing data sets without the computational overhead and infrastructure necessary to run a full land model. Here, we introduce the capabilities of the testbed by using a single realization of climate and plant productivity estimates that serve as common inputs to each of three soil organic matter models. In the subsections that follow, we describe each component of the biogeochemical testbed in

greater detail, but briefly outline the workflow and configuration of the model here (Figure 1).

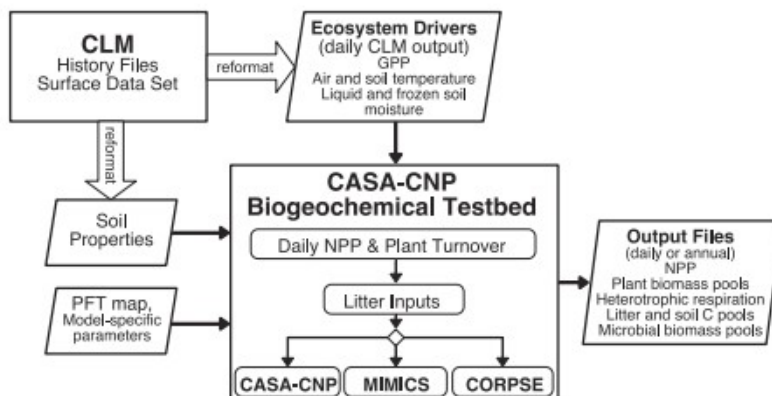


FIGURE 1 Configuration of the biogeochemical testbed. Inputs required by the testbed include daily estimates of gross primary productivity (GPP), air temperature, soil temperature, and soil moisture as well as static maps of soil properties and vegetation types. For the simulations presented here these were generated by simulations from the Community Land Model forced with CRU-NCEP climate reanalyses for the period 1901–2010, but other input streams can be used in the testbed. From these inputs the CASA-CNP vegetation model calculates daily NPP and litterfall fluxes, which are delivered to each of the soil biogeochemical models. Output from the testbed include daily and annually averaged carbon stocks and fluxes for vegetation and soils

Daily estimates of GPP, air temperature, soil temperature, and soil moisture are needed as inputs to the testbed. The simulations presented here used data from the Community Land Model (CLM version 4.5, discussed below). Inputs force the Carnegie-Aimes-Stanford Approach terrestrial biosphere model (CASA-CNP; created by Potter et al., 1993), with modifications by (Randerson, Thompson, Conway, Fung, & Field, 1997; Randerson, Thompson, Malmstrom, Field, & Fung, 1996); and with N and P biogeochemistry as implemented by (Wang, Law, & Pak, 2010). Here, we use the carbon-only version of CASA-CNP vegetation model to calculate net primary productivity (NPP) and carbon allocation to different plant tissues (roots, wood, and leaves), as well as the timing of litterfall. Litterfall inputs are passed onto three different soil biochemical models that include the CASA-CNP model that implicitly represents microbial activity using a first-order decomposition approach, as well as two recently developed microbially explicit models that include the Microbial-Mineralization Carbon Stabilization model (MIMICS; Wieder, Grandy, Kallenbach, & Bonan, 2014; Wieder, Grandy, Kallenbach, Taylor, & Bonan, 2015) and the Carbon, Organisms, Rhizosphere, and Protection in the Soil Environment model (CORPSE; Sulman, Phillips, Oishi, Shevliakova, & Pacala, 2014). For each model, we ran a spin up simulation to bring soil organic matter pools to steady state and then conducted a transient simulation including changes in climate and NPP over the historical period (1901–2010) to compare the stocks and changes of soil C pools simulated by each soil model. Below we summarize the data inputs, CASA-CNP vegetation model, the three soil carbon models applied in the testbed, and the testbed configuration. More detailed information can be found in the online user's manual and technical documentation that accompanies the

publically available model testbed code available at github.com/wwieder/biogeochem_testbed_1.0.

2.1 Data inputs

Data inputs for the biogeochemical testbed can be modified from a variety of sources, but for this study, data inputs were generated by the CLM using a satellite phenology scheme forced with the CRU-NCEP climate reanalysis (Koven et al., 2013; Oleson et al., 2013; Figure 1). This standard configuration of CLM generated globally gridded daily output of gross primary productivity (GPP), air temperature, soil temperature, liquid soil moisture and frozen soil moisture for the historical period (1901–2010). Soil texture inputs to the testbed were depth-weighted means in the top 50 cm of soil from the CLM surface data set (Oleson et al., 2013). The testbed assigned a single plant functional type (PFT) to each $2^\circ \times 2^\circ$ grid cell, computed as the mode from the 1-km International Geosphere–Biosphere Program Data and Information System (IGBP DISCover) data set with 18 vegetation types, including grassy tundra (Loveland et al., 2000; National Center for Atmospheric Research Staff, 2017). CASA-CNP defines biome-specific parameters corresponding to each PFT (Table S1). Results presented here use output from the two-degree version of CLM as input to the testbed, although the testbed operates independent of resolution and can even be configured to run for a single point or field site. Postprocessing of CLM history files was required to format input data that could be read into the testbed. Specifically, average soil temperature and liquid and frozen soil moisture used by the testbed are depth-weighted means in the rooting zone according to the PFT-specific root depth and root distribution (Table S1). Only liquid soil moisture was considered when computing soil moisture limits on growth for the vegetation model and decomposition in the CASA-CNP and CORPSE soil models. CORPSE also required information on frozen soil moisture to calculate air-filled pore space. MIMICS did not consider soil moisture effects on decomposition.

2.2 CASA-CNP vegetation model

The carbon-only version of the CASA-CNP terrestrial biosphere model calculated daily net primary production (NPP) and subsequent plant litter inputs to the soil. Daily NPP was calculated by subtracting the sum of plant maintenance and growth respiration from the CLM-derived GPP. Maintenance respiration in CASA-CNP was zero for leaves, and calculated as a function of N content ($\text{g C g N}^{-1} \text{ day}^{-1}$) for wood and fine roots (determined from fixed biome-specific C:N ratios, Table S1). These respiration rates were zero for air/soil temperatures $\leq 250 \text{ K}$ and increased exponentially with temperature using a fixed biome-specific Q_{10} (Sitch et al., 2003). Growth respiration was a fixed fraction (0.35) of the quantity GPP minus the sum of maintenance respiration fluxes. The relative amounts of NPP allocated to leaves, wood, or fine roots were fixed biome-specific fractions that depended on leaf phenology phase (Wang et al., 2010).

Turnover of live leaves, wood, and fine roots occurred daily at biome-specific age-related death rates. The leaf turnover rate increased with cold and drought stress, and was modeled following the approach of (Arora & Boer, 2005). Nonwoody plant litter was partitioned into structural and metabolic litter material as a function of the biome-specific lignin:N ratio of the plant litter (Table S1). Woody plant litter accumulated in the coarse woody debris (CWD) pool, which decomposed as a function of temperature and soil moisture for all models and included CO₂ respiration loss. Metabolic litter, structural litter, and decomposing CWD comprised C inputs to all soil carbon models in the testbed.

2.3 Soil carbon models

Previous publications document soil models applied in the testbed, but Table 1 summarizes some of the key similarities and differences among the soil models. Additional details are also available in the user's manual and technical documentation available in the testbed's GitHub repository (see Acknowledgements). The CASA-CNP soil carbon model had two litter pools (metabolic and structural) and three soil organic matter pools (fast, slow, and passive). Live microbial biomass was not explicitly simulated as a driver of decomposition, but the transfer of C from litter to soil pools or among soil carbon pools produced CO₂ respiration losses. The decomposition of pool *i* (D_i) is controlled pools size (C_i) and pool specific first-order kinetics (k_i) that are modified by environmental scalars calculated as a function of soil temperature and moisture (T and θ , respectively).

$$D_i = C_i \cdot k_i \cdot f(T) \cdot f(\theta) \quad (1)$$

TABLE 1 Comparison of key features distinguishing the soil models implemented in the biogeochemical testbed. The list here is not intended to be exhaustive, see relevant publications and the online user's manual and technical documentation for more information

	CASA-CNP	MIMICS	CORPSE
Microbial representation	Implicit with first order kinetics	Explicit, with two microbial functional groups	Explicit, with one microbial pool in each litter and soil layer (including rhizosphere vs. bulk soils)
Litter carbon pools	2 + coarse woody debris	2	3, assumed to be above the soil mineral surface
Soil carbon pools	3	3	6, assumed to be in the mineral soil
Kinetics	First order linear	Reverse Michaelis-Menten	Reverse Michaelis-Menten
Temperature function	Exponential function of soil temperature	Temperature dependent V_{max} & K_{es}	Temperature dependent V_{max} (Arrhenius function)
Soil moisture function	Bell-shaped curve with maximum at 55% total water saturation	None	Bell-shaped curve with maximum at 55% liquid water saturation, greater moisture limitation at high and low soil moisture
Vertical resolution	1 layer for biogeochemistry	1 layer (0–100 cm) for biogeochemistry	2 layers: mineral soil (0–100 cm) and litter layer
Soil texture effects on SOC protection	Finely textured soil increases transfer coefficients to passive pool	Clay content increases the allocation to, and slows the turnover of "physically protected" SOM	Clay content increases transfers from unprotected soil pools to their protected counterparts
Nutrients	C, N, P, C-only version used here	C-only model	C-only model
References	Wang et al. (2010)	Wieder, Grandy, et al. (2014), Wieder, Grandy, et al. (2015)	Sulman et al. (2014)

Structural and metabolic litter pools decomposed into fast and slow pools as a function of lignin fraction. The CWD pool decomposed to the fast and slow SOM pools also as a function of the wood lignin fraction. Transfers of C from the fast and slow pools formed the passive pool and were a function of soil texture. The passive pool decomposed without transfers of C to other pools. In CASA-CNP the cropland PFTs had no moisture limitation on soil organic matter decomposition and daily turnover rates for the fast, slow, and passive pools were multiplied by 1.25, 1.5, and 1.5 respectively. Neither MIMICS nor CORPSE modified decomposition rates for croplands.

MIMICS had two litter pools (metabolic and structural), two live microbial biomass pools (copiotrophic and oligotrophic, referred to as *r* and *K*, respectively), and three soil organic matter pools (available, chemically protected, and physically protected). Nonwoody plant litter was partitioned into metabolic and structural litter pools using a slightly different function of the lignin:N ratio than the one in the CASA-CNP model (see user's manual). Decomposing CWD carbon was transferred to the structural litter pool. The microbial decomposition of metabolic and structural litter and available SOM pools were controlled by reverse Michaelis-Menten kinetics and modified by soil temperature:

$$D_i = V_{\max_{r/K}}(T) \cdot C_i \frac{MIC_{r/K}}{K_{es_{r/K}}(T) + MIC_{r/K}} \quad (2)$$

where D_i was the decomposition of pool i , $V_{\max}(T)$ was the temperature-sensitive maximum reaction velocity, $K_{es}(T)$ was the temperature-sensitive half-saturation constant specific to the *r* or *K* microbial pool, C_i was the carbon pool, and $MIC_{r/K}$ was the *r* or *K* microbial pool. Decomposition fluxes also controlled the growth of microbial biomass pools and had CO_2 respiration losses that were determined by fixed (flux-specific) microbial growth efficiencies. Microbial turnover, which was proportional to annual NPP, transferred C to physically protected, chemically protected, and available SOM pools, without CO_2 respiration loss. Desorption of the physically protected pool followed first-order kinetics and was described as a function of soil clay content, without CO_2 loss. Oxidation of the chemically protected SOM, which transferred C to the available pool, followed reverse Michaelis-Menten kinetics and was therefore dependent on the size of standing microbial biomass pools, but as none of the carbon is assimilated into microbial biomass there are no associated CO_2 losses.

CORPSE had separate surface litter layer pools and SOM pools, each with three chemically defined carbon species (labile, chemically resistant, and dead microbes) and a live microbial biomass pool. The surface litter pools were all considered unprotected while the SOM pools had unprotected and protected counterparts. Metabolic and structural leaf litter was transferred to the labile and chemically resistant surface litter pools, respectively, without CO_2 respiration losses. Similarly, metabolic and structural root litter was transferred to labile and chemically resistant unprotected soil carbon pools,

respectively. Root exudates, calculated as a fixed 2% of NPP, also contributed to the labile unprotected soil pool. We reduced root litter input by the amount of root exudate C added so total C inputs to CORPSE were identical to those of the other soil models. Carbon from the decomposing CWD pool was transferred to the chemically resistant litter pool. No carbon was transferred between the surface litter and soil layers. The microbial decomposition of unprotected labile, chemically resistant, and dead microbe litter and SOM pools, CO₂ fluxes, and the growth of microbial biomass were controlled by the existing microbial biomass and modified by soil temperature and moisture:

$$D_i = V_{max,i}(T) \cdot \left(\frac{\theta}{\theta_{sat}}\right)^3 \left(1 - \frac{\theta}{\theta_{sat}}\right)^{2.5} \cdot C_i \frac{MIC}{MIC + Kes \times \sum_j C_j} \quad (3)$$

where θ was volumetric liquid soil water content and θ_{sat} was saturation soil water content. Microbial growth efficiencies used fixed, pool-specific fractions, with labile C having a high associated growth efficiency and chemically resistant C having a low efficiency. The model assumed that the microbial biomass limitation on decomposition was related to the microbial biomass as a fraction of total carbon. As a result, decomposition rate responded linearly to total carbon content (similar to a first-order model) but was accelerated by greater labile C inputs (which stimulated microbial biomass growth) and suppressed when labile C was depleted relative to chemically resistant C. Microbial turnover, which was proportional to a fixed turnover rate, transferred C to the unprotected dead microbes pool, with CO₂ respiration loss. Carbon was transferred at fixed, first-order rates from the unprotected soil pools to their protected counterparts. These rates varied with clay content and chemical species (with dead microbes having a relatively higher protection rate), and occurred without CO₂ respiration losses. Protected C was transferred back to unprotected pools at a different fixed, first order rate.

2.4 Testbed configuration, simulations, & analyses

The simulations for each SOM model were carried out in three steps: initialization, spinup, and transient simulations, which are described below. We initialized CASA-CNP vegetation pools by running the testbed with 1901 forcings for 100 years. This initialization created more stable vegetation pools and litter inputs for subsequent simulations. The state of the CASA-CNP vegetation pools (but not SOM pools) from this initialization simulation were used to initialize spinup runs for all SOM models.

Soil carbon pools were spun up by cycling over 1901–1920 forcings until organic matter pools reached equilibrium. An SOM model was considered to be in equilibrium when all three of the following criteria were met between 20-year cycles: global litter plus soil carbon stocks changed <0.01 Pg, total litter plus soil carbon in >98% of grid cells changed <1 g C/m², and total litter plus soil carbon in >98% of grid cells changed <0.1%. Spinup times

varied between models. CASA-CNP required 10,000 years of an accelerated spinup followed by 10,000 years of normal spinup in order to reach equilibrium. For the accelerated spinup, the decomposition rate of the passive pool was increased tenfold. Following accelerated spinup, the passive carbon stock was multiplied tenfold before starting the normal spinup phase. MIMICS organic matter pools required 12,000 years to reach equilibrium, with the physically protected pool requiring the longest spinup time. CORPSE organic matter pools required 50,000 years to reach equilibrium, primarily due to slow continuing accumulation of chemically resistant litter in high latitudes. In all models, these spinup times are still prohibitively long for doing many repeated simulations or parameter estimation, and highlight a research priority that must be addressed (Luo et al., 2016) in this and other work.

We conducted full transient simulations from 1901 to 2010. For each of the three soil models currently implemented in the testbed, we compared: (1) initial conditions following model spinup; (2) changes in soil carbon pools over the transient simulation; and (3) seasonal patterns of heterotrophic respiration. Here, we focus on total soil carbon stocks that are simulated by each model, which were calculated as the sum of all litter, microbial biomass, and soil carbon pools. Beyond initial carbon stocks, estimates of steady-state soil carbon turnover times provide a metric to evaluate the emergent relationship between climate the mean residence time of various C stocks (Koven, Hugelius, Lawrence, & Wieder, 2017). Recognizing that turnover times vary with model structure in transient simulations (Rasmussen et al., 2016), turnover times were calculated by dividing initial soil carbon stocks by heterotrophic respiration fluxes for each model, masking out points with initial productivity $<100 \text{ g C m}^{-2} \text{ year}^{-1}$. Simulated results were compared to an observationally derived functional relationship with mean annual temperature from Koven et al. (2017) that was calculated by dividing soil carbon stocks from the Harmonized World Soils Database (HWSD; FAO et al., 2012) and Northern Circumpolar Soil Carbon Database (Hugelius et al., 2013) by MODIS NPP estimates (Zhao, Heinsch, Nemani, & Running, 2005). Although this turnover time vs. climate relationship is derived from present day estimates of plant productivity, we contend that these inferred turnover times represent important global-scale patterns that models should be expected to replicate.

Several additional experiments were conducted that demonstrate the utility of the testbed in rapidly assessing and understanding variation among models. Initial simulations suggested that soil texture potentially mediated soil C responses among models. Thus, we repeated the spinup and fully transient simulations with globally consistent soil texture (20% clay, 40% silt, and 40% sand). This global loam experiment only changed the soil texture effects on particular transfer coefficients and turnover times that were simulated by each soil biogeochemical model and did not concurrently modify the soil hydraulic conditions. Second, to decompose the effects of

particular forcings on soil carbon stocks we conducted three isolated-forcing experiments where plant productivity, soil temperature, and soil moisture individually changed over the 20th century, but the remaining input variables were held constant (cycling over 1901–1920 values as in the spinup). We compared the time series of soil carbon changes from isolated forcing experiments to the fully transient 20th century simulations.

3 RESULTS

3.1 Initial conditions

When forced with CRU-NCEP climate, simulated global mean annual soil temperatures were 15.6°C and mean liquid soil moisture was 42.1% of saturation (Figure S1a,b, averaged over the initialization period, 1901–1920). GPP estimates from CLM4.5sp totaled 117 ± 1.1 Pg C/year (mean $\pm 1 \sigma$) and initial NPP estimates from CASA-CNP averaged 48 ± 0.8 Pg C/year (Figure S2a). With these inputs, the biogeochemical testbed generated total carbon stocks (including litter, soil organic matter and microbial biomass) totaling 1,360, 1,420, and 1,410 Pg carbon for CASA-CNP, MIMICS, and CORPSE respectively (Figure 2a–c; Figure S3). For comparison, soil C estimates from the HWSD totaled 1,260 Pg C globally (Figure 2d; 0–100 cm depth, as regridded by (Wieder, Boehnert, Bonan, & Langseth, 2014). Our aim here is not to evaluate the spatial distribution of soil carbon stocks simulated by any of the models, although the testbed offers opportunities for parameter estimation in single point and global simulations (e.g., Hararuk, Smith, & Luo, 2015). We note, however, that MIMICS was calibrated against the HWSD (Wieder, Grandy, et al. 2015), whereas CASA-CNP and CORPSE were not similarly calibrated. We also recognize that global stocks of ‘litter’ C are not clearly defined in globally gridded soil carbon estimates, and that the HWSD likely underestimates high latitude soil C stocks (Todd-Brown et al., 2013). Thus, we also present permafrost soil C estimates from the NCSCD (0–100 cm depth), which shows larger soil carbon stocks in permafrost regions (Figure 3, Figure S3). The three soil models implemented in the testbed adequately represented global soil carbon stocks, falling within benchmark ranges for global soil carbon stocks given an observationally consistent field of plant productivity (Todd-Brown et al., 2014).

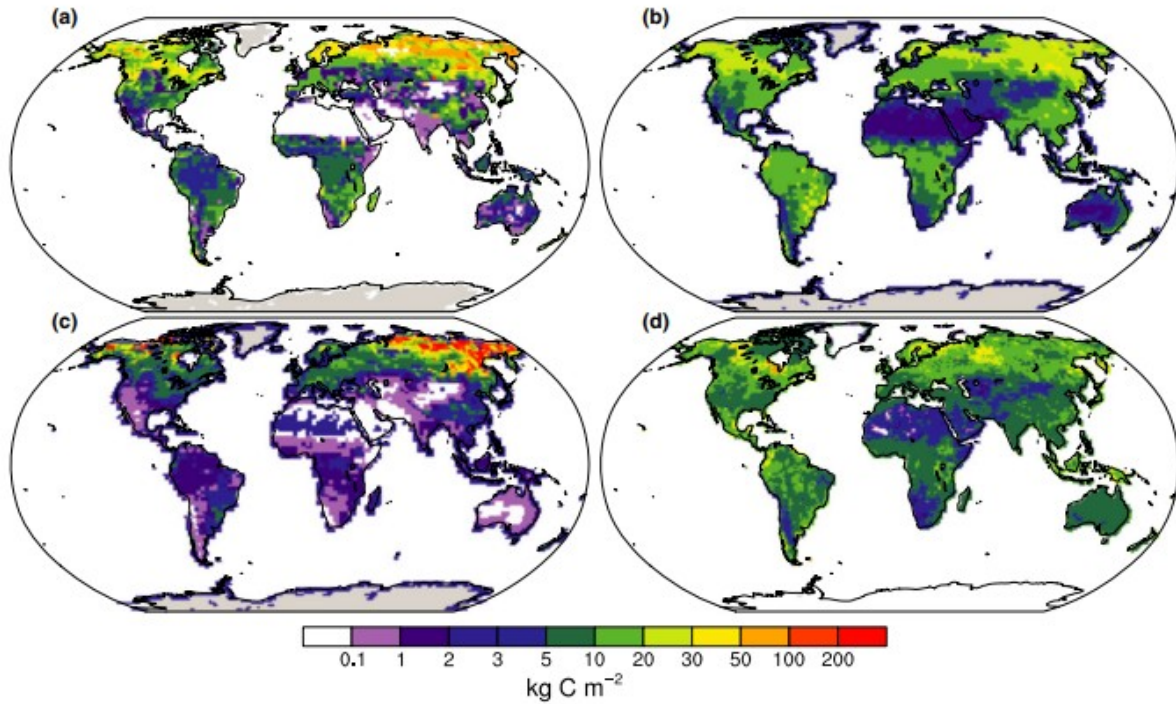


FIGURE 2 Steady state soil carbon stocks (kg C/m^2) simulated in the biogeochemical testbed for (a) CASA-CNP, 1,360 Pg C; (b) MIMICS, 1,420 Pg C; (c) CORPSE, 1,410 Pg C; and (d) the HWSD observations, 1,260 Pg C. All values represent the sum of litter, soil, and microbial biomass carbon that are averaged over the initialization period (1901–1920; 0–100 cm depth for MIMICS, CORPSE, and HWSD). Note, that MIMICS was previously calibrated against the HWSD and the quasi-logarithmic scale bar

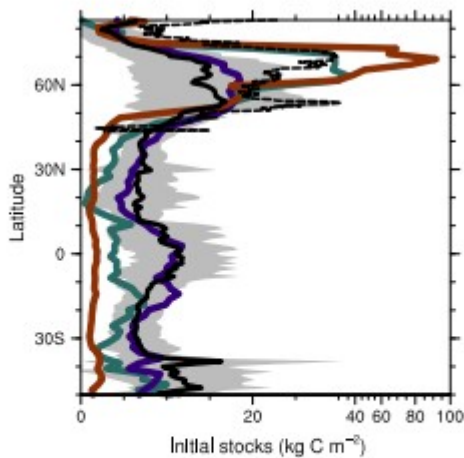


FIGURE 3 Zonal mean of steady state soil carbon stocks (kg C/m^2) calculated for each latitude band for CASA-CNP (green line), MIMICS (purple line) CORPSE (brown line), the HWSD observations (solid black line $\pm 1 \sigma$, shaded area), and the NCSCD observations (dashed black line) Note irregular spacing on the x-axis

Despite general agreement of global soil C stocks among models, they exhibited notably different spatial distributions. Across high latitudes, CASA-

CNP and CORPSE generated steady-state soil C densities that were closer to observations from the NCSCD and notably larger than those simulated by MIMICS or observed in the HWSD (Figures 2 and 3, Figure S3). Conversely, at low latitudes, CASA-CNP and CORPSE displayed soil carbon densities well below estimates from MIMICS and the HWSD. The global loam experiment indicated that steady-state carbon stocks simulated in CASA-CNP and MIMICS showed a greater sensitivity to soil texture (-95 and -178 Pg C, respectively, compared to control simulation) than CORPSE ($+ 27$ Pg C). Whereas CASA-CNP showed relatively homogenous reductions in steady-state soil carbon stocks, MIMICS showed substantially larger soil C differences in regions of high clay content (e.g., much of the tropics, the southeastern United States, and SE Asia, Figure S4). All three models generally showed larger carbon stocks in tundra regions with loam soils, especially CORPSE.

Although the soil models used similar temperature functions, they showed large differences in patterns of inferred turnover times and temperature (Figure 4). Models and observations showed the longest turnover times in grid cells with colder mean annual temperatures. Observations suggested that over the cold domain (mean annual temperature $<0^{\circ}\text{C}$) soil carbon turnover had a higher temperature sensitivity (steeper slope), whereas over the warm domain (mean annual temperature $>15^{\circ}\text{C}$) turnover times had a lower temperature sensitivity (shallow slope; Koven et al., 2017). The CASA-CNP soil model simulated a log-linear relationship between temperature and the logarithm of turnover time, with variation among individual grid cells largely attributed to differences in soil moisture (Figure 4a). In the cold domain, CASA-CNP matched the higher temperature sensitivity of soil carbon turnover better than the two microbially explicit models. In warmer sites, however, CASA-CNP showed a linear decrease in log turnover times (especially in mesic and wet systems), that was not consistent with observation-based estimates. (The cluster of grid cells with very low turnover times are agricultural grid cells, mainly in India, that had high productivity, but very low soil carbon stocks owing to how agricultural decomposition rates are handled in CASA-CNP). By contrast, MIMICS failed to represent high temperature sensitivity in the cold-domain, but over the warm-domain MIMICS captured the lower temperature sensitivity (flat slope) of inferred turnover times, although the intercept may be too high (Figure 4b). Finally, CORPSE showed a stronger than observed temperature sensitivity in all cases (Figure 4c), with long turnover times simulated by CORPSE in the cold-domain resulting in large carbon stocks at high latitudes. Thus, despite similarities in the overall soil C stocks represented by these models we find strong differences in the spatial distribution and potential temperature sensitivities among CASA, MIMICS, and CORPSE that may influence projections of soil carbon change over the historical period.

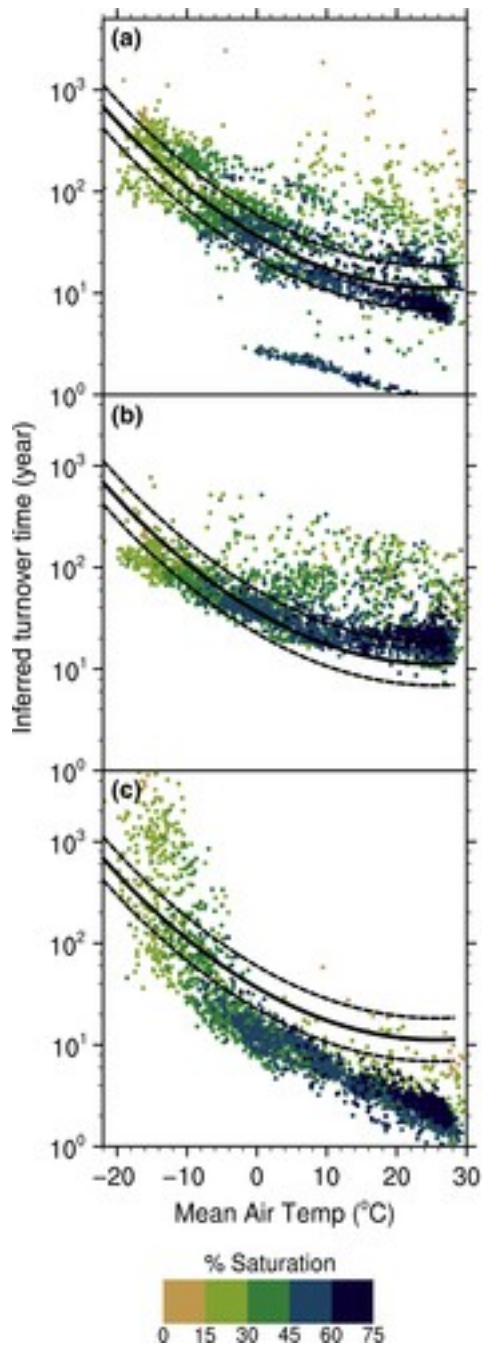


Figure 4

Inferred soil carbon turnover times vs. mean annual temperature for each grid cell in CASA-CNP, MIMICS, and CORPSE (a-c respectively). Points are colored by mean annual soil moisture (percent saturation of liquid water), and binned according to the color bar below the figure. Black lines show the observationally derived relationship between inferred turnover times and temperature $\pm 50\%$ prediction interval (calculated by Koven et al., 2017)

3.2 Transient response

By the end of the transient simulation period, global mean annual soil temperature increased by 1.1°C and mean annual soil moisture (calculated as percent saturation) increased by 0.5%, relative to the initial conditions

(Figure 5a). Notably, high latitude soils showed the greatest changes, generally becoming warmer and wetter (Figure S1c-d), with higher wintertime soil temperatures increasing liquid water availability for longer periods of time. By the start of the 21st century, GPP increased by 19 Pg C/year (+16%); meanwhile NPP increased 7 Pg C/year (+15%; Figure 5a; Figure S2b), and similar in magnitude to an ensemble of CMIP5 Earth system models (Wieder, Cleveland, Smith, & Todd-Brown, 2015). Higher plant productivity increased global vegetation carbon stocks simulated by CASA-CNP by 36 Pg C, whereas coarse woody debris stocks declined by 0.7 Pg C.

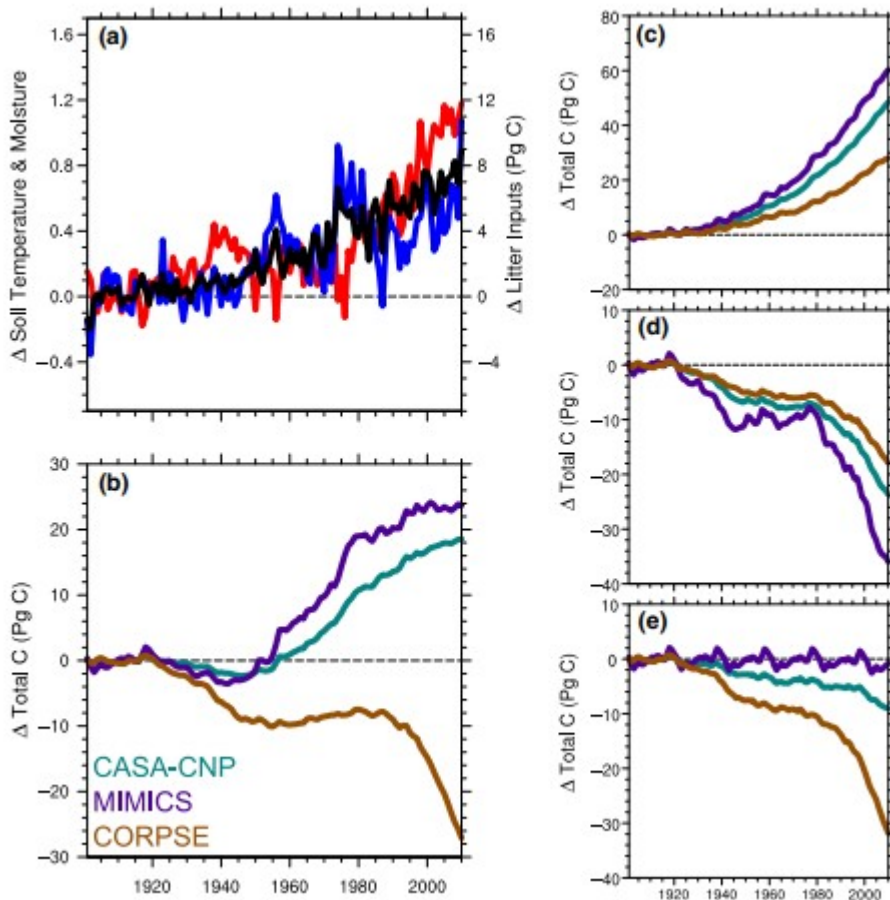


Figure 5

Globally averaged changes in (a) environmental conditions: soil temperature (°C), soil moisture (% saturation), and plant litter inputs (red, blue and black lines, respectively); and the cumulative change (b) soil carbon stocks simulated by: CASA-CNP, MIMICS, and CORPSE (green, purple, and brown lines, respectively) in the full transient simulation. Isolated forcing experiments showing changes in soil carbon stocks following changes in only (c) GPP, (d) soil temperature, and (e) soil moisture. For all plots, annual values were weighted by land area and differenced from initial conditions averaged over the spin-up period

Changes in productivity and climate drove a net accumulation of soil carbon in CASA-CNP and MIMICS by the end of the simulation (+18.1 and +24.1 Pg C, respectively), whereas CORPSE lost soil carbon over the same period

(−21.7 Pg C; Figure 5b). Despite receiving identical litter inputs and climate forcing, the three soil models tested here showed dramatically different spatial patterns of soil carbon gains and losses (Figure 6). Particular changes in soil carbon stocks largely depended on the balance of changes in plant productivity and soil conditions, along with different assumptions made by each model. For example, in tundra ecosystems plant productivity increased by 20%–30%, whereas soil temperature warmed by <math><1^{\circ}\text{C}</math> (Figures S1 and S2). In CASA-CNP and MIMICS this increased plant productivity overwhelmed soil carbon losses from the increased heterotrophic respiration, leading to net soil carbon accumulations – mainly in the litter pools simulated by both models. By contrast, CORPSE lost large amounts of soil carbon in these regions (Figure 6). Soil texture largely modulated the initial soil carbon stocks simulated by each model (Figure S4), but had a more muted effect on transient soil C dynamics. In the global loam experiment, soil carbon accumulations in CASA-CNP and MIMICS were dampened (+17.7 and +19.0 Pg C, respectively), whereas CORPSE lost slightly more soil carbon over the same period (−22.1 Pg C). MIMICS assumed that clay rich soils preferentially stabilize microbial residues in physically protected soil organic matter pools; thus, in the global loam experiment soil carbon accumulations were approximately 200 g C/ m² (roughly 20%) less across the tropics in MIMICS (data not shown).

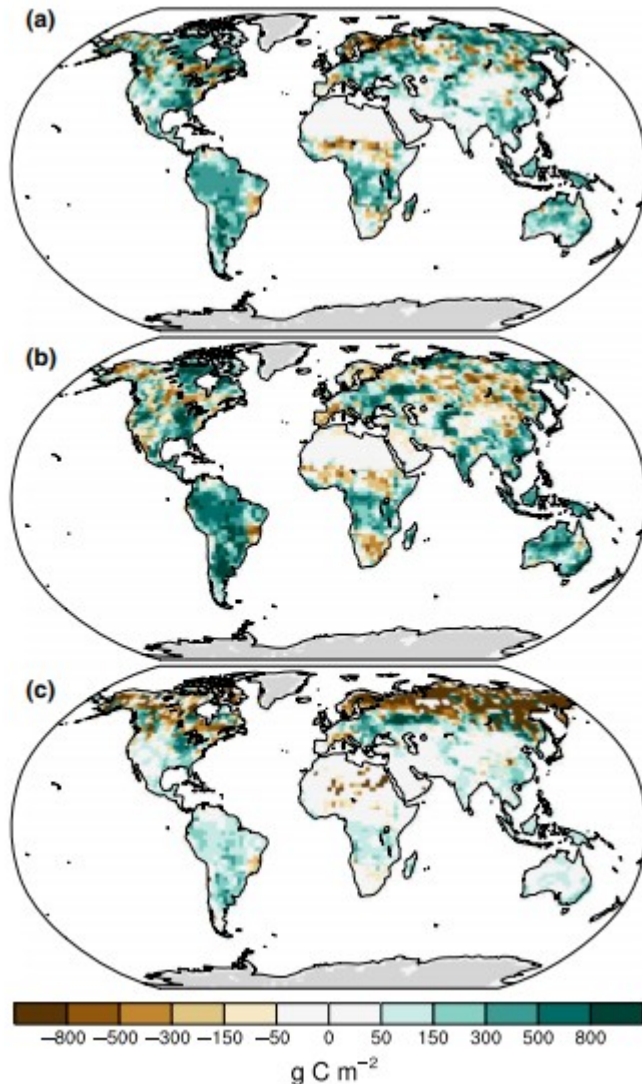


Figure 6

Spatial distribution of changes in soil carbon stocks (g C/m^2) simulated by the end of the historical period (mean of 2001-2010) in the biogeochemical testbed for (a) CASA-CNP (+18 Pg C), (b) MIMICS (+24 Pg C), and (c) CORPSE (-21 Pg C)

The testbed allowed us to parse out gross changes among models from isolated forcing experiments, rather than just seeing the net changes over the fully transient simulation. Isolated forcing experiments showed that MIMICS had a higher sensitivity to changes in plant productivity and temperature than the other models—accumulating twice the amount of C as CORPSE in the isolated GPP experiment, and losing twice as much C in the isolated soil temperature simulation (Figure 5c,d, Figure S5). Most of these differences, however, took place in mid-to-low latitudes ($<50^\circ\text{N}$), where MIMICS simulated significantly larger initial carbon stocks than the other two models (Figure 3). In MIMICS, microbial turnover increased with higher plant productivity (Wieder, Grandy, et al. 2015). This served as a density dependent control over decomposition rates (Buchkowski, Bradford, Grandy,

Schmitz, & Wieder, 2017), but it also increased the inputs of microbial residues to soil organic matter pools.

Our transient simulations highlighted uncertainties in understanding temperature and moisture sensitivity in cold regions. Warmer temperatures ultimately drove the high latitude soil C losses simulated over the 20th century; but the isolated forcing experiments demonstrated that CASA-CNP and MIMICS had stronger direct sensitivities to changing temperatures (Figures 5 and 6, Figure S5). By contrast, CORPSE showed the largest sensitivity to isolated soil moisture forcings (including thawing of frozen soil water), and lost more than three times the amount of C as the comparable CASA-CNP simulation (Figure 5e, Figure S5). Nearly all of the simulated C losses came from high latitude ecosystems—where soil moisture changes are mainly controlled by freeze/thaw state and the thawing of frozen soils allowed the large C stocks built up in frozen conditions to decompose. Thus, actual temperature sensitivity may be a combination of metabolic sensitivities to temperature, as well as interactions between temperature and moisture via controls over liquid water availability in soils subject to freezing (Commane et al., 2017; Koven, Lawrence, & Riley, 2015).

To further explore differences among models we looked at mean annual cycles of heterotrophic respiration from the testbed (Figure 7). By design, at the beginning of the simulations litter inputs equaled heterotrophic respiration rates for all models (48.1 Pg C/year). A climatology of annual soil respiration rates averaged across latitudinal bands, therefore, illustrates differences in the seasonal cycle of carbon fluxes from each model. As each soil model in the testbed was driven by a common climate and vegetation model, differences among the left panels of Figure 7 reflect distinctions in the seasonal amplitude of terrestrial net ecosystem exchange with the atmosphere. Across midlatitudes in the northern hemisphere CASA-CNP showed the lowest amplitude in seasonal CO₂ fluxes (Figure 7a). Over this same region, MIMICS showed higher summertime respiration than CASA-CNP, but both models simulated similar wintertime respiration rates (Figure 7c). By contrast, CORPSE had very low midlatitude heterotrophic respiration fluxes in winter, but much larger summertime rates—generating the highest amplitude seasonal cycle of all the models (Figure 7e). The stronger seasonal cycle shown by CORPSE is consistent with the high transient sensitivity to freeze/thaw state by that model. These distinctions were amplified over time (Figure 7, right panels), showing a global intensification of heterotrophic CO₂ fluxes between the first and last decades of the simulation. By the end of the transient simulation annual CO₂ fluxes were no longer equal among models, however, as soil carbon losses were greater for CORPSE, which simulated heterotrophic respiration fluxes that were roughly 1 Pg C/year higher than CASA-CNP and MIMICS. By the end of the transient simulations, we also note a qualitative difference in the latitude-seasonal responses of HR between CORPSE and the other models in the mid- to high- latitude regions, where CORPSE tends to show respiratory increases earlier in the season and

more northerly than the baseline climatological cycle, while the other two models tend to show increases that are more closely aligned in seasonality and latitude with the baseline climatology (Figure 7b,d,f).

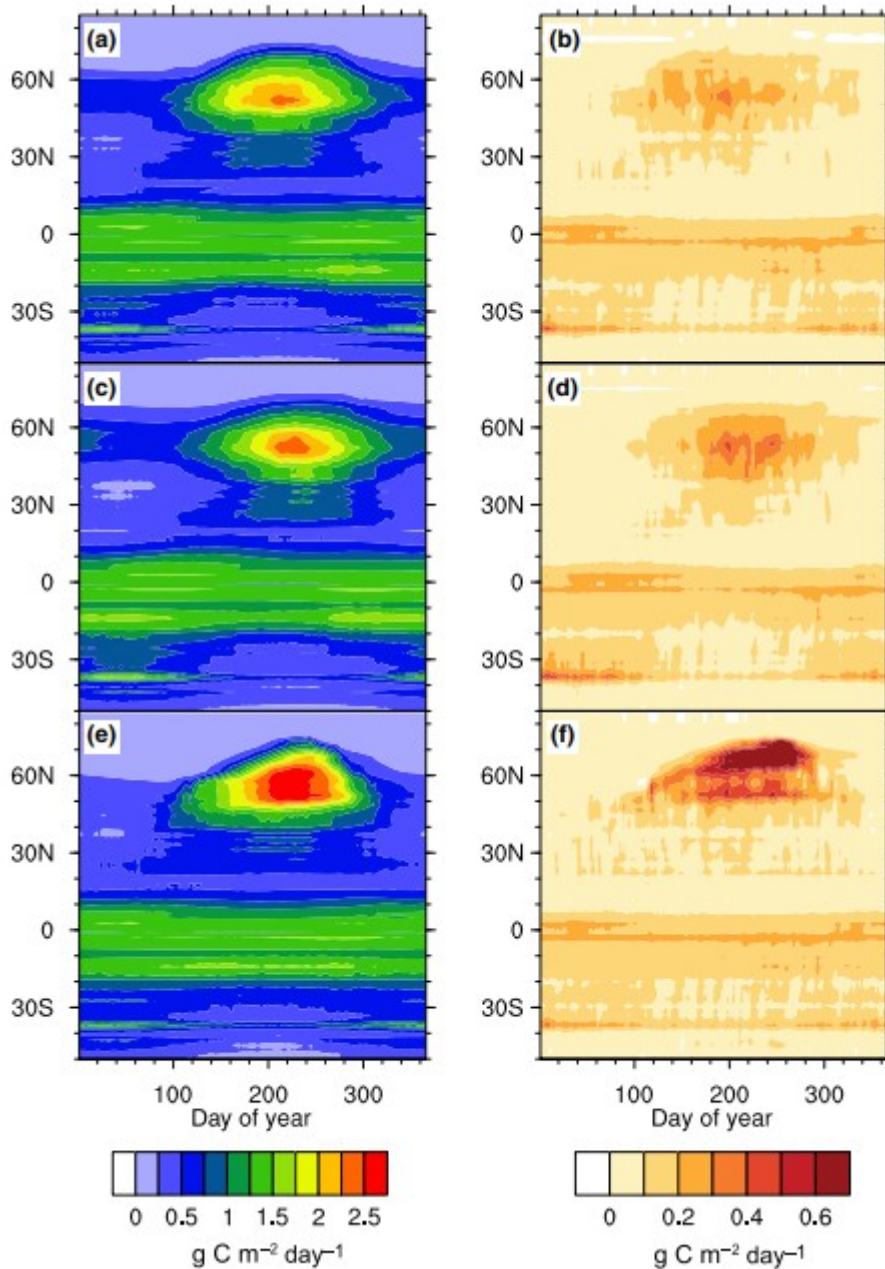


Figure 7

Hovmöller diagram showing the climatological mean daily respiration rate (g C m⁻² day⁻¹) averaged over each latitude band for the initialization period (1901-1920; left column), and the difference between the final (2001-2010) and initial (1901-1920) mean daily respiration rates (right column). Results from each model are shown for (a, b) CASA-CNP, (c, d) MIMICS, and (e, f) CORPSE

To clarify differences among models we focused on fluxes from a single latitudinal band (here 54°N) over the last decade of the simulation.

Figure 8 illustrates the seasonal cycle of environmental drivers (temperature, soil moisture, and litter inputs), as well as the annual evolution of heterotrophic respiration fluxes and microbial biomass represented by each model. Again, CASA-CNP and MIMICS produced similar wintertime fluxes. With warming in spring (and greater availability of liquid water) heterotrophic respiration rates quickly accelerated in all models, but this occurs sooner in the year for both CASA-CNP and CORPSE (Figure 8). The annual respiration rates simulated by CASA-CNP generally tracked soil temperature changes, with maximum fluxes corresponding to periods with the warmest soil temperatures. By contrast, the maximum respiration rates simulated by the microbially explicit models were somewhat lagged from the CASA-CNP fluxes—corresponding to periods when litter inputs and temperature were also highest. Moreover, MIMICS and CORPSE both simulated higher maximum heterotrophic respiration rates, leading to a higher amplitude in the seasonal cycle of soil CO₂ fluxes. Some of this temporal shift in respiration rates was likely related to changes in microbial biomass stocks, which broadly tracked the seasonal cycle of litter inputs.

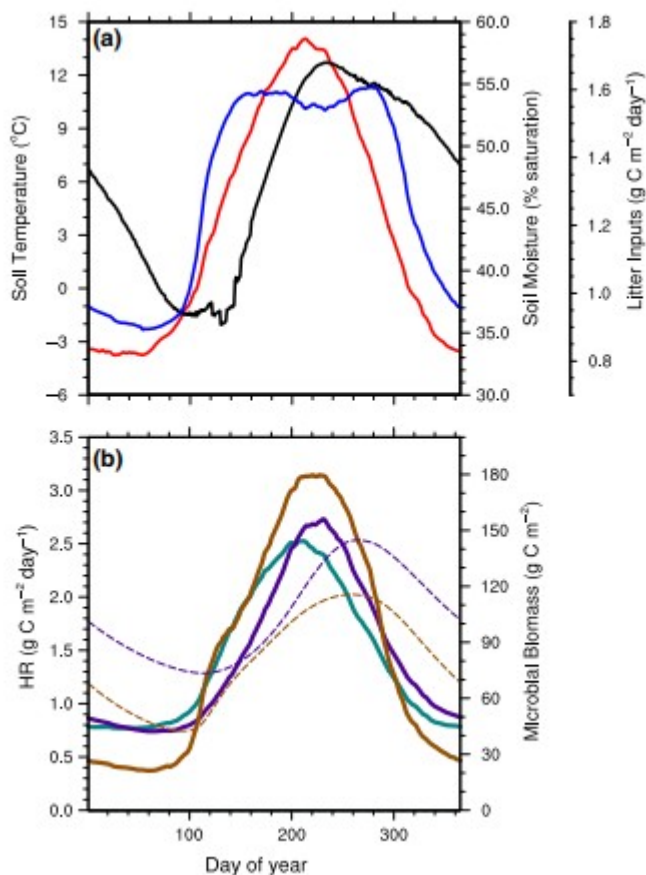


Figure 8

Mean annual cycle of (a) soil temperature, soil moisture and litter inputs (red, blue, and black lines, respectively) at 54°N over the last decade of the simulation (2001–2010). The lower panel (b) shows heterotrophic respiration fluxes (solid lines) and microbial biomass stocks (dashed lines) from CASA-

CNP, MIMICS, and CORPSE (green, purple, and brown lines, respectively) for the same region and time period

4 DISCUSSION

Our results suggest that the actual uncertainty related to soil carbon projections may be larger than previously realized. Todd-Brown et al. (2013, 2014) reported a wider range of initial soil carbon stocks and trajectories over the 21st century from an ensemble of CMIP5 models, but each of these models was forced with spatially varying and highly model-idiosyncratic climate and productivity estimates. By using a consistent forcing among models, our results better capture the variation in soil carbon stocks and their potential response to environmental change that is caused by different model assumptions, which is translated into model structures, and particular model parameterizations. Indeed, given their common forcing, global similarities in testbed results are not surprising (Ahlström, Schurgers, Arneeth, & Smith, 2012; Friend et al., 2014). Models in the biogeochemical testbed, however, more broadly sample the theoretical space related to soil organic matter decomposition and stabilization (Wieder, Allison, et al. 2015). This variation in model form (and parameterization) translated into differences among models in the: distribution of steady state soil carbon stocks (Figures 2 and 3); functional relationship of turnover time with mean annual temperature (Figure 4); transient response of soil carbon stocks to environmental perturbations (Figures 5 and 6) and seasonal dynamics of heterotrophic respiration (Figures 7 and 8). We acknowledge that some model spread is likely explained by differences in calibration approaches; specifically, MIMICS was calibrated against the global pattern of C stocks estimated by HWSO, while CORPSE and CASA-CNP were not (Figure 2). Future calibration of all three models against the same benchmark (e.g., Figure 4) may reduce uncertainty in the transient responses among models (Figure 5).

Through the historical period, CASA-CNP and MIMICS show similar changes in global soil carbon stocks (+18 and +24 Pg C, respectively), which were opposite in sign from the soil carbon changes simulated by CORPSE (-21 Pg C; Figure 5). When combined with changes to vegetation C stocks from the CASA-CNP simulations (+36 Pg C) projected terrestrial carbon uptake would fall well short of terrestrial carbon sink estimated by the Global Carbon Project (62–142 Pg C between 1959–2010, assuming uncertainty of 0.8 Pg C/year; Houghton et al., 2012; Le Quéré et al., 2014). Although our simulations lack representation of land use and land cover change, results from the testbed demonstrate that in order to capture inferred trends in terrestrial carbon uptake over the end of the 20th century much less carbon would have to accumulate in vegetation pools of land models that applied CASA-CNP and MIMICS than would be necessary in a model using CORPSE. Here, we focus on understanding the structural uncertainties among models that broadly relate to differences among models in their representation of physicochemical stabilization of soil organic matter, temperature

sensitivities, and moisture sensitivities. Notably, we found that uncertainties regarding the physicochemical stabilization of soil organic matter and freeze-thaw dynamics were greater than uncertainties related to direct temperature sensitivities among models.

4.1 Physicochemical stabilization

Physical limitation of microbial access to otherwise decomposable substrates plays a critical role in preserving soil organic matter (Conant et al., 2011; Cotrufo, Wallenstein, Boot, Deneff, & Paul, 2013; Dungait, Hopkins, Gregory, & Whitmore, 2012; Lehmann & Kleber, 2015; Schimel & Schaeffer, 2012). Concurrently, microbial biomass serves as both the catalyst for soil organic matter decomposition and the source of soil organic matter formation, through the mineral stabilization of microbial residues and necromass (Grandy & Neff, 2008; Kallenbach, Frey, & Grandy, 2016; Liang, Cheng, Wixon, & Balser, 2011). While the three models included in the testbed all represented this process, their implementations and assumptions differed substantially, reflecting important uncertainties in how to appropriately represent pore-scale physicochemical stabilization mechanisms in global-scale models. Our global loam experiment illustrated that steady-state soil carbon dynamics in CASA-CNP and MIMICS showed a greater sensitivity to soil texture than CORPSE (Figure S4). While the appropriateness of soil texture to describe diverse stabilization mechanisms on mineral surfaces and within aggregates is in itself debatable (Doetterl et al., 2015; Mikutta, Kleber, Torn, & Jahn, 2006), texture still serves as a useful proxy for which gridded input data sets are available for global-scale simulations (Bailey et al., 2017). We also note that few of the ESMs represented in the CMIP5 archive use any information about edaphic properties (texture, mineralogy, or pH) in their soil biogeochemical submodels.

Regional differences in initial soil carbon stocks highlight the need to better resolve factors regulating physicochemical stabilization of soil organic matter in models. For example, CASA-CNP and CORPSE simulated lower than observed steady-state soil carbon densities in warmer ecosystems (Figures 2 and 3). This suggests that the physicochemical stabilization mechanisms implicitly represented in these models may not be strong enough to counteract environmental conditions that would otherwise favor rapid decomposition (Figure 4). By contrast, MIMICS simulated higher soil carbon stocks in warm regions that were more consistent with observation-based estimates. Similarly, variation among models in transient simulations reflects uncertainty related to the ultimate fate of new carbon that enters terrestrial ecosystems. In first order models, like CASA-CNP, variation in carbon inputs largely determines the variation in soil carbon changes, reflecting the linear relationship between inputs and turnover times (Koven, Chambers, et al., 2015; Todd-Brown et al., 2014). Accordingly, increased productivity in the transient simulation increased soil carbon stocks in CASA-CNP, especially in colder climates with longer base turnover times (Figures 5c and 6a, Figure S5b). In the microbially explicit models, increased

plant productivity and litter inputs also build proportionally larger microbial biomass pools (Figure S2c-d). These larger microbial biomass pools can simultaneously accelerate the decomposition of organic matter and build soil carbon stocks. The balance of these factors depends on assumptions about the catalytic capacity of larger microbial biomass pools vs. the potential fate of microbial residues.

Increased plant productivity over the 20th century increased the rate at which microbial residues contributed to soil organic matter pools. MIMICS assumes that finely textured soils have a much greater capacity to stabilize microbial residues (Wieder, Grandy, et al., 2014), accounting for the larger tropical soil C accumulation (Figure 6b, Figure S5b). In contrast, larger microbial biomass pools simulated by CORPSE (as well as increased root exudation) accelerated the decomposition of unprotected soil organic matter and litter stocks resulting in smaller increases in C stocks globally (Figures 5c and 6c). The rapid turnover times simulated by CORPSE in temperate and tropical ecosystems (Figure 4) suggest that little of the new carbon will be retained in CORPSE simulations, an interpretation supported by results from the isolated GPP simulation (Figure S5b).

Indeed, losses of soil carbon have been observed with increasing plant productivity in high-latitude ecosystems (Hartley et al., 2012). In temperate forests, multidecadal litter manipulation studies generally show modest carbon accumulation in organic soil horizons, but no change in the carbon stocks of mineral soils (Bowden et al., 2014; Lajtha, Bowden, & Nadelhoffer, 2014; Lajtha, Townsend, et al., 2014). This suggests a more nuanced relationship between plant productivity and soil carbon storage may be necessary to understand and simulate likely terrestrial carbon responses to changes in plant productivity. The models in the biogeochemical testbed take a step in this direction, but our results highlight the need to refine the representation of factors affecting microbial access to otherwise decomposable substrates in soils.

4.2 Temperature sensitivities

Uncertainties in observed soil biogeochemical responses to temperature present notable challenges for projecting terrestrial carbon dynamics in a warming world (Conant et al., 2011; Davidson & Janssens, 2006; Jones, Cox, & Huntingford, 2003). Although theory predicts that warmer temperatures should accelerate soil organic matter decomposition and lead to soil carbon losses, experimental evidence for these assumptions remains unclear (Bradford, Wieder, et al., 2016). Recent syntheses, however, demonstrate that experimental warming consistently increases soil respiration rates (Carey et al., 2016) and leads to soil carbon losses in sites where initial soil carbon stocks were large (Crowther et al., 2016). Models in the testbed reflected these general expectations (Figure 5), but extending the insight provided from these relatively short-term experimental findings to decadal- and centennial-scales increases the uncertainty associated with societally

relevant carbon cycle projections. Moreover, these syntheses cannot decompose the changes in productivity vs. turnover times associated with warming; however, they do corroborate field studies suggesting that warmer summertime temperature may be accelerating the decomposition of soil organic matter in the Alaskan tundra and thereby turning Arctic landscapes into a source of carbon dioxide to the atmosphere (Commane et al., 2017; Schuur et al., 2009). Collectively, these observations highlight the importance of capturing the appropriate soil carbon temperature sensitivity for understanding potential carbon cycle - climate feedbacks, especially in carbon-rich, high latitude ecosystems.

Differences in base decomposition rates and temperature sensitivities largely describe differences in steady state and transient responses among first-order models (Todd-Brown et al., 2014), but understanding apparent temperature response functions that emerge from microbially explicit models is somewhat more complicated. Decomposition rates of organic matter in MIMICS and CORPSE were controlled by reverse Michaelis-Menten based kinetics (Equations 2 and 3), and both models applied temperature functions to calculate maximum reaction velocities (V_{\max}) with similar temperature sensitivities (Q_{10} , data not shown). MIMICS, however, also calculates a temperature sensitive half-saturation constant (K_{es}). This likely dampened the climate sensitivity of soil carbon turnover times (German, Marcelo, Stone, & Allison, 2012) and decreased the apparent Q_{10} of simulated reaction rates (Davidson & Janssens, 2006). These factors may explain the shallow slope in the MIMICS log turnover time - temperature relationships in warmer domains (Figure 4b). By contrast, CORPSE used a fixed half-saturation constant, applied an Arrhenius equation to calculate V_{\max} (resulting in higher temperature sensitivities at lower temperatures), and assumed that the chemical quality of different substrate pools conferred different temperature sensitivities. Additionally, CORPSE strongly limited decomposition when soil water was mostly frozen while MIMICS did not include an explicit soil moisture dependence. As a result, the inferred turnover times simulated by CORPSE in temperate and tropical ecosystems were very fast, but a strong moisture limitation to decomposition rates in frozen soils drove the change in slope of the log turnover times with air temperature in Figure 4c.

Model structure also determines variation in the transient responses among models (Jones et al., 2005; Rasmussen et al., 2016). For example, steady state turnover times simulated by MIMICS showed the lowest temperature sensitivity (Figure 4), but the model also had the largest soil C losses in the isolated soil warming experiment (Figure 5d); whereas the opposite was true for CORPSE. At high latitudes, most soil carbon simulated by MIMICS was in pools that were vulnerable to microbial degradation and, therefore, sensitive to changes in temperature (Figure 5d, Figure S5c). By contrast, much of the soil carbon simulated by CASA-CNP was in pools with slower decomposition rates, thus extending the time needed for temperature sensitivities to

emerge. Indeed, previous work indicates that over decadal times scales MIMICS has a faster response to experimental warming, compared to a first order model, but over centennial time scales ultimately loses less carbon (Wieder, Grandy, et al., 2014). Moreover, local effects like edaphic properties, substrate quality, microbial community composition, soil moisture, and redox conditions compound uncertainty in assessing the vulnerability of soil carbon stocks to temperature change (Bradford, Berg, Maynard, Wieder, & Wood, 2016; Bradford et al., 2014; Davidson & Janssens, 2006). Interactions between soil moisture and temperature resulted in more modest C losses from CORPSE in the isolated soil temperature experiment (Figure 5d,e; discussed next). Articulating the true uncertainty associated with any projection of soil carbon change, therefore, requires a deeper investigation into the structural assumptions represented in models—which extends beyond temperature sensitivity of carbon turnover times.

4.3 Moisture sensitivities

At multiple scales of interest, measuring and modeling soil water availability remains highly uncertain (Clark et al., 2015; Loescher, Ayres, Duffy, Luo, & Brunke, 2014). Subsequently, translating the effects of the soil hydrologic state into biogeochemical models also presents enormous challenges (Carvalhais et al., 2014; Manzoni & Katul, 2014; Moyano, Manzoni, & Chenu, 2013). Yet, water availability fundamentally determines microbial activity in all soils. Limited liquid water availability notably preserves soil organic matter in high-latitude permafrost systems, where soil water can be frozen for most or all of the year. The transition from liquid to frozen water rapidly reduces decomposition rates in the field (Commane et al., 2017) and models (Koven, Lawrence, et al., 2015), albeit with varied sensitivities (Figure 5e). Because it lacks structures that consider the effects of liquid water availability on decomposition rates, MIMICS simulated rapid turnover times and low soil carbon stocks in permafrost regions (Figures 3 and 4b). In contrast, CORPSE was especially sensitive to freezing because it strongly limited decomposition at low soil moisture (Equation 3; Sulman et al., 2014). This accentuated the strong threshold behavior in steady state turnover times around mean annual temperatures of 0°C (Figure 4c) and resulted in much lower wintertime respiration fluxes from CORPSE (Figures 7 and 8).

We recognize that the abrupt changes in turnover times with frozen soils reflected in CORPSE simulations are at least partially due to the single-layer implementation of the soil models here. Indeed, all of the models may benefit from explicitly resolving profiles of soil temperature and moisture in their representation of biogeochemical processes to better capture permafrost soil carbon dynamics (Koven et al., 2013, 2017). Nevertheless, lengthening of the nonfrozen season in permafrost soils has been shown to significantly increase soil carbon emissions (Commane et al., 2017); and these contrasting model outcomes (Figures 5 and 6) highlight real and important sources of uncertainty in projecting carbon cycle responses to

warming and associated hydrologic changes, especially at high latitudes. The results from CORPSE projecting larger global soil carbon changes to soil moisture (which is mainly an indirect temperature effect) than to the direct temperature effect, as well as the larger disagreement between CORPSE and the other models in the testbed for moisture than temperature responses (Figures 5e and 6, Figure S5), underscores both the importance and lack of model agreement on this critical process. Again, however, finding appropriate data streams to parameterize soil moisture effects on substrate availability for a global-scale model remains a challenge. More broadly, uncertainties among models and observational data sets related to permafrost soil carbon densities and vulnerability to environmental change remain an outstanding challenge for global-scale models (Burke, Jones, & Koven, 2013; Koven, Riley, & Stern, 2012; Koven, Lawrence, et al., 2015) that reflects the difficulty in representing interactions between the physical soil systems and the biotic agents responsible for soil organic matter formation and decomposition.

This work addresses a particular challenge in comparing, evaluating and ultimately improving global-scale soil biogeochemical models under a common experimental framework. The biogeochemical testbed provides a computationally tractable, numerically consistent framework to begin exploring the effects of different model structures and parameterizations on soil carbon stocks and fluxes at global scales. Variation in soil carbon projections among models were caused by differences in the steady state turnover times simulated by each model, and the turnover time responses to environmental changes over the 20th century. These can be simplified into uncertainties among models related to the physicochemical stabilization limiting microbial access to otherwise decomposable carbon substrates, temperature sensitivities of soil organic matter turnover, and effects of liquid water availability on microbial activity. An important application of the testbed is motivating improvements in model structures and parameterizations. Based on our initial results we suggest that improved parameterization of temperature sensitivities in CORPSE and implementation of water availability effects on decomposition (especially in frozen soils) in MIMICS could improve the fidelity of simulations using those models. Moreover, none of the carbon-only, single layer models implemented in the testbed consider the effects of vertical resolution in regulating SOM turnover—highlighting gaps that should be addressed with future model development. Continuing to resolve these key uncertainties will require greater communication between empirical and modeling communities. As models begin to more faithfully reflect theoretical understanding of factors responsible for soil organic matter formation and decomposition we see the testbed as a tool to facilitate regional- to global-scale model comparison and evaluation, while developing understanding of soil biogeochemical processes.

ACKNOWLEDGEMENTS

The testbed model code, user's manual and technical documentation are publically available at github.com/wwieder/biogeochem_testbed_1.0. This work was supported by the US Department of Energy, Office of Science, Biological and Environmental Research (BER) under award numbers TES DE-SC0014374 and BSS DE-SC0016364, US Department of Agriculture NIFA 2015-67003-23485, and US Department of Energy-Biological and Environmental Research, RUBISCO SFA. B. Sulman was supported under award NA14OAR4320106 from the National Oceanic and Atmospheric Administration, U.S. Department of Commerce. The statements, findings, conclusions, and recommendations are those of the author(s) and do not necessarily reflect the views of the National Oceanic and Atmospheric Administration, or the U.S. Department of Commerce.

References

- Ahlström, A., Schurgers, G., Arneth, A., & Smith, B. (2012). Robustness and uncertainty in terrestrial ecosystem carbon response to CMIP5 climate change projections. *Environmental Research Letters*, 7, 044008. <https://doi.org/10.1088/1748-9326/7/4/044008>
- Anav, A., Friedlingstein, P., Kidston, M., Bopp, L., Ciais, P., Cox, P., ... Zhu, Z. (2013). Evaluating the land and ocean components of the global carbon cycle in the CMIP5 earth system models. *Journal of Climate*, 26, 6801– 6843. <https://doi.org/10.1175/jcli-d-12-00417.1>
- Arora, V. K., & Boer, G. J. (2005). A parameterization of leaf phenology for the terrestrial ecosystem component of climate models. *Global Change Biology*, 11, 39– 59. <https://doi.org/10.1111/j.1365-2486.2004.00890.x>
- Arora, V. K., Boer, G. J., Friedlingstein, P., Eby, M., Jones, C. D., Christian, J. R., ... Hajima, T. (2013). Carbon-concentration and carbon-climate feedbacks in CMIP5 earth system models. *Journal of Climate*, 26, 5289– 5314. <https://doi.org/10.1175/jcli-d-12-00494.1>
- Bailey, V. L., Bond-Lamberty, B., Deangelis, K., Grandy, A. S., Hawkes, C. V., Heckman, K., ... Wallenstein, M. D. (2017). Soil carbon cycling proxies: Understanding their critical role in predicting climate change feedbacks. *Global Change Biology*, 1– 11. <https://doi.org/10.1111/gcb.13926>
- Bowden, R. D., Deem, L., Plante, A. F., Peltre, C., Nadelhoffer, K., & Lajtha, K. (2014). Litter input controls on soil carbon in a temperate deciduous forest. *Soil Science Society of America Journal*, 78, S66– S75. <https://doi.org/10.2136/sssaj2013.09.0413nafsc>
- Bradford, M. A., Berg, B., Maynard, D. S., Wieder, W. R., & Wood, S. A. (2016). Understanding the dominant controls on litter decomposition. *Journal of Ecology*, 104, 229– 238. <https://doi.org/10.1111/1365-2745.12507>
- Bradford, M. A., & Fierer, N. (2012). The biogeography of microbial communities and ecosystem processes: Implications for soil and ecosystem

models. In D. H. Wall, R. D. Bardget, V. Behan-Pelletier, J. E. Herrick, T. H. Jones, K. Ritz, J. Six, D. R. Strong & W. H. Van Der Putten (Eds.), *Soil ecology and ecosystem services* (pp. 189– 200). Oxford, UK: Oxford University Press. <https://doi.org/10.1093/acprof:oso/9780199575923.003.0017>

Bradford, M. A., Warren li, R. J., Baldrian, P., Crowther, T. W., Maynard, D. S., Oldfield, E. E., ... King, J. R. (2014). Climate fails to predict wood decomposition at regional scales. *Nature Climate Change*, 4, 625– 630. <https://doi.org/10.1038/nclimate2251>

Bradford, M. A., Wieder, W. R., Bonan, G. B., Fierer, N., Raymond, P. A., & Crowther, T. W. (2016). Managing uncertainty in soil carbon feedbacks to climate change. *Nature Climate Change*, 6, 751– 758. <https://doi.org/10.1038/nclimate3071>

Buchkowski, R. W., Bradford, M. A., Grandy, A. S., Schmitz, O. J., & Wieder, W. R. (2017). Applying population and community ecology theory to advance understanding of belowground biogeochemistry. *Ecology Letters*, 20, 231– 245. <https://doi.org/10.1111/ele.12712>

Burke, E. J., Jones, C. D., & Koven, C. D. (2013). Estimating the permafrost-carbon climate response in the CMIP5 climate models using a simplified approach. *Journal of Climate*, 26, 4897– 4909. <https://doi.org/10.1175/jcli-d-12-00550.1>

Carey, J. C., Tang, J., Templer, P. H., Kroeger, K. D., Crowther, T. W., Burton, A. J., ... Jiang, L. (2016). Temperature response of soil respiration largely unaltered with experimental warming. *Proceedings of the National Academy of Sciences of the USA*, 113, 13797– 13802. <https://doi.org/10.1073/pnas.1605365113>

Carvalhais, N., Forkel, M., Khomik, M., Bellarby, J., Jung, M., Migliavacca, M., ... Weber, U. (2014). Global covariation of carbon turnover times with climate in terrestrial ecosystems. *Nature*, 514, 213– 217. <https://doi.org/10.1038/nature13731>

Ciais, P., Sabine, C., Bala, G., Bopp, L., Brovkin, V., Canadell, J., ... Jones, C. (2013). Carbon and other biogeochemical cycles. In T. F. Stocker, D. Qin, G.-K. Plattner, M. Tignor, S. K. Allen, J. Boschung, A. Nauels, Y. Xia, V. Bex & P. M. Midgley (Eds.), *Climate change 2013: The physical science basis. Contribution of Working Group I to the Fifth Assessment Report of the Intergovernmental Panel on Climate Change* (pp. 465– 570). Cambridge, UK and New York, NY, USA: Cambridge University Press.

Clark, M. P., Nijssen, B., Lundquist, J. D., Kavetski, D., Rupp, D. R., Woods, R. A., ... Arnold, J. R. (2015). A unified approach for process-based hydrologic modeling: 1. Modeling concept. *Water Resources Research*, 51, 2498– 2514. <https://doi.org/10.1002/2015WR017198>

Commane, R., Lindaas, J., Benmergui, J., Luus, K. A., Chang, R., Daube, B. C., ... Miller, S. M. (2017). Carbon dioxide sources from Alaska driven by

increasing early winter respiration from Arctic tundra. *Proceedings of the National Academy of Sciences of the USA*, 114, 5361– 5366. <https://doi.org/10.1073/pnas.1618567114>

Conant, R. T., Ryan, M. G., Ågren, G. I., Birge, H. E., Davidson, E. A., Eliasson, P. E., ... Hyvönen, R. (2011). Temperature and soil organic matter decomposition rates – Synthesis of current knowledge and a way forward. *Global Change Biology*, 17, 3392– 3404. <https://doi.org/10.1111/j.1365-2486.2011.02496.x>

Cotrufo, M. F., Wallenstein, M. D., Boot, C. M., Deneff, K., & Paul, E. (2013). The Microbial Efficiency-Matrix Stabilization (MEMS) framework integrates plant litter decomposition with soil organic matter stabilization: Do labile plant inputs form stable soil organic matter? *Global Change Biology*, 19, 988– 995. <https://doi.org/10.1111/gcb.12113>

Crowther, T. W., Todd-Brown, K. E. O., Rowe, C. W., Wieder, W., Carey, J. C., Machmuller, M. B., ... Blair, J. M. (2016). Quantifying global soil carbon losses in response to warming. *Nature*, 540, 104– 108. <https://doi.org/10.1038/nature20150>

Davidson, E. A., & Janssens, I. A. (2006). Temperature sensitivity of soil carbon decomposition and feedbacks to climate change. *Nature*, 440, 165– 173. <https://doi.org/10.1038/nature04514>

Doetterl, S., Stevens, A., Six, J., Merckx, R., Van Oost, K., Pinto, M. C., ... Boeckx, P. (2015). Soil carbon storage controlled by interactions between geochemistry and climate. *Nature Geoscience*, 8, 780– 783. <https://doi.org/10.1038/ngeo2516>

Dungait, J. J., Hopkins, D. W., Gregory, A. S., & Whitmore, A. P. (2012). Soil organic matter turnover is governed by accessibility not recalcitrance. *Global Change Biology*, 18, 1781– 1796. <https://doi.org/10.1111/j.1365-2486.2012.02665.x>

Exbrayat, J. F., Pitman, A. J., & Abramowitz, G. (2014). Disentangling residence time and temperature sensitivity of microbial decomposition in a global soil carbon model. *Biogeosciences*, 11, 6999– 7008. <https://doi.org/10.5194/bg-11-6999-2014>

FAO, IIASA, ISRIC, ISSCAS, JRC (2012). *Harmonized world soil database (version 1.2)*. Rome, Italy: FAO; and Laxenburg, Austria: IIASA.

Friedlingstein, P., Meinshausen, M., Arora, V. K., Jones, C. D., Anav, A., Liddicoat, S. K., & Knutti, R. (2014). Uncertainties in CMIP5 climate projections due to carbon cycle feedbacks. *Journal of Climate*, 27, 511– 526. <https://doi.org/10.1175/jcli-d-12-00579.1>

Friend, A. D., Lucht, W., Rademacher, T. T., Keribin, R., Betts, R., Cadule, P., ... Ito, A. (2014). Carbon residence time dominates uncertainty in terrestrial vegetation responses to future climate and atmospheric CO₂. *Proceedings of*

the National Academy of Sciences of the USA, 111, 3280– 3285. <https://doi.org/10.1073/pnas.1222477110>

German, D. P., Marcelo, K. R. B., Stone, M. M., & Allison, S. D. (2012). The Michaelis-Menten kinetics of soil extracellular enzymes in response to temperature: A cross-latitudinal study. *Global Change Biology*, 18, 1468– 1479. <https://doi.org/10.1111/j.1365-2486.2011.02615.x>

Grandy, A. S., & Neff, J. C. (2008). Molecular C dynamics downstream: The biochemical decomposition sequence and its impact on soil organic matter structure and function. *Science of the Total Environment*, 404, 297– 307. <https://doi.org/10.1016/j.scitotenv.2007.11.013>

Hararuk, O., Smith, M. J., & Luo, Y. (2015). Microbial models with data-driven parameters predict stronger soil carbon responses to climate change. *Global Change Biology*, 21, 2439– 2453. <https://doi.org/10.1111/gcb.12827>

Hartley, I. P., Garnett, M. H., Sommerkorn, M., Hopkins, D. W., Fletcher, B. J., Sloan, V. L., ... Wookey, P. A. (2012). A potential loss of carbon associated with greater plant growth in the European Arctic. *Nature Climate Change*, 2, 875– 879. <https://doi.org/10.1038/nclimate1575>

Hoffman, F. M., Randerson, J. T., Arora, V. K., Bao, Q., Cadule, P., Ji, D., ... Obata, A. (2014). Causes and implications of persistent atmospheric carbon dioxide biases in earth system models. *Journal of Geophysical Research: Biogeosciences*, 119, 141– 162. <https://doi.org/10.1002/2013JG002381>

Houghton, R. A., House, J. I., Pongratz, J., Van Der Werf, G. R., DeFries, R. S., Hansen, M. C., ... Ramankutty, N. (2012). Carbon emissions from land use and land-cover change. *Biogeosciences*, 9, 5125– 5142. <https://doi.org/10.5194/bg-9-5125-2012>

Hugelius, G., Tarnocai, C., Broll, G., Canadell, J. G., Kuhry, P., & Swanson, D. K. (2013). The Northern Circumpolar Soil Carbon Database: Spatially distributed datasets of soil coverage and soil carbon storage in the northern permafrost regions. *Earth System Science Data*, 5, 3– 13. <https://doi.org/10.5194/essd-5-3-2013>

Jobbágy, E. G., & Jackson, R. B. (2000). The vertical distribution of soil organic carbon and its relation to climate and vegetation. *Ecological Applications*, 10, 423– 436. [https://doi.org/10.1890/1051-0761\(2000\)010\[0423:tvdoso\]2.0.co;2](https://doi.org/10.1890/1051-0761(2000)010[0423:tvdoso]2.0.co;2)

Jones, C. D., Ciais, P., Davis, S. J., Friedlingstein, P., Gasser, T., Peters, G. P., ... Jackson, R. B. (2016). Simulating the Earth system response to negative emissions. *Environmental Research Letters*, 11, 095012. <https://doi.org/10.1088/1748-9326/11/9/095012>

Jones, C. D., Cox, P., & Huntingford, C. (2003). Uncertainty in climate-carbon-cycle projections associated with the sensitivity of soil respiration to

temperature. *Tellus Series B*, 55, 642– 648. <https://doi.org/10.1034/j.1600-0889.2003.01440.x>

Jones, C., McConnell, C., Coleman, K., Cox, P., Falloon, P., Jenkinson, D., & Powlson, D. (2005). Global climate change and soil carbon stocks; predictions from two contrasting models for the turnover of organic carbon in soil. *Global Change Biology*, 11, 154– 166. <https://doi.org/10.1111/j.1365-2486.2004.00885.x>

Jones, C., Robertson, E., Arora, V., Friedlingstein, P., Shevliakova, E., Bopp, L., ... Liddicoat, S. (2013). Twenty-first-century compatible CO₂ emissions and airborne fraction simulated by CMIP5 earth system models under four representative concentration pathways. *Journal of Climate*, 26, 4398– 4413. <https://doi.org/10.1175/jcli-d-12-00554.1>

Kallenbach, C. M., Frey, S. D., & Grandy, A. S. (2016). Direct evidence for microbial-derived soil organic matter formation and its ecophysiological controls. *Nature Communications*, 7, 13630. <https://doi.org/10.1038/ncomms13630>

Koven, C. D., Chambers, J. Q., Georgiou, K., Knox, R., Negron-Juarez, R., Riley, W. J., ... Jones, C. D. (2015). Controls on terrestrial carbon feedbacks by productivity versus turnover in the CMIP5 earth system models. *Biogeosciences*, 12, 5211– 5228. <https://doi.org/10.5194/bg-12-5211-2015>

Koven, C. D., Hugelius, G., Lawrence, D. M., & Wieder, W. R. (2017). Higher climatological temperature sensitivity of soil carbon in cold than warm climates. *Nature Climate Change*, 7, 817– 822. <https://doi.org/10.1038/nclimate3421>

Koven, C. D., Lawrence, D. M., & Riley, W. J. (2015). Permafrost carbon–climate feedback is sensitive to deep soil carbon decomposability but not deep soil nitrogen dynamics. *Proceedings of the National Academy of Sciences of the USA*, 112, 3752– 3757. <https://doi.org/10.1073/pnas.1415123112>

Koven, C. D., Riley, W. J., & Stern, A. (2012). Analysis of permafrost thermal dynamics and response to climate change in the CMIP5 earth system models. *Journal of Climate*, 26, 1877– 1900. <https://doi.org/10.1175/jcli-d-12-00228.1>

Koven, C. D., Riley, W. J., Subin, Z. M., Tang, J. Y., Torn, M. S., Collins, W. D., ... Swenson, S. C. (2013). The effect of vertically-resolved soil biogeochemistry and alternate soil C and N models on C dynamics of CLM4. *Biogeosciences*, 10, 7109– 7131. <https://doi.org/10.5194/bg-10-7109-2013>

Lajtha, K., Bowden, R. D., & Nadelhoffer, K. (2014). Litter and root manipulations provide insights into soil organic matter dynamics and

stability. *Soil Science Society of America Journal*, 78, S261- S269. [10.2136/sssaj2013.08.0370nafsc](https://doi.org/10.2136/sssaj2013.08.0370nafsc)

Lajtha, K., Townsend, K. L., Kramer, M. G., Swanston, C., Bowden, R. D., & Nadelhoffer, K. (2014). Changes to particulate versus mineral-associated soil carbon after 50 years of litter manipulation in forest and prairie experimental ecosystems. *Biogeochemistry*, 119, 341- 360. <https://doi.org/10.1007/s10533-014-9970-5>

Le Quéré, C., Peters, G. P., Andres, R. J., Andrew, R. M., Boden, T. A., Ciais, P., ... Sitch, S. (2014). Global carbon budget 2013. *Earth System Science Data*, 6, 235- 263. <https://doi.org/10.5194/essd-6-235-2014>

Lehmann, J., & Kleber, M. (2015). The contentious nature of soil organic matter. *Nature*, 528, 60- 68. <https://doi.org/10.1038/nature16069>

Liang, C., Cheng, G., Wixon, D., & Balser, T. (2011). An Absorbing Markov Chain approach to understanding the microbial role in soil carbon stabilization. *Biogeochemistry*, 106, 303- 309. <https://doi.org/10.1007/s10533-010-9525-3>

Loescher, H., Ayres, E., Duffy, P., Luo, H., & Brunke, M. (2014). Spatial variation in soil properties among North American ecosystems and guidelines for sampling designs. *PLoS One*, 9, e83216. <https://doi.org/10.1371/journal.pone.0083216>

Loveland, T. R., Reed, B. C., Brown, J. F., Ohlen, D. O., Zhu, Z., Yang, L., & Merchant, J. W. (2000). Development of a global land cover characteristics database and IGBP DISCover from 1 km AVHRR data. *International Journal of Remote Sensing*, 21, 1303- 1330. <https://doi.org/10.1080/014311600210191>

Luo, Y. Q., Ahlstrom, A., Allison, S. D., Batjes, N. H., Brovkin, V., Carvalhais, N., ... Georgiou, K. (2016). Toward more realistic projections of soil carbon dynamics by earth system models. *Global Biogeochemical Cycles*, 30, 40- 56. <https://doi.org/10.1002/2015gb005239>

Manzoni, S., & Katul, G. (2014). Invariant soil water potential at zero microbial respiration explained by hydrological discontinuity in dry soils. *Geophysical Research Letters*, 41, 7151- 7158. <https://doi.org/10.1002/2014GL061467>

Manzoni, S., & Porporato, A. (2009). Soil carbon and nitrogen mineralization: Theory and models across scales. *Soil Biology and Biochemistry*, 41, 1355- 1379. <https://doi.org/10.1016/j.soilbio.2009.02.031>

Mikutta, R., Kleber, M., Torn, M., & Jahn, R. (2006). Stabilization of soil organic matter: Association with minerals or chemical recalcitrance? *Biogeochemistry*, 77, 25- 56. <https://doi.org/10.1007/s10533-005-0712-6>

Moyano, F. E., Manzoni, S., & Chenu, C. (2013). Responses of soil heterotrophic respiration to moisture availability: An exploration of processes and models. *Soil Biology and Biochemistry*, 59, 72– 85. <https://doi.org/10.1016/j.soilbio.2013.01.002>

National Center for Atmospheric Research Staff (Eds). (2017). The climate data guide: CERES: IGBP land classification. Retrieved from <https://climatedataguide.ucar.edu/climate-data/ceres-igbp-land-classification>

Oleson, K., Lawrence, D. M., Bonan, G. B., Drewniak, B., Huang, M., Koven, C., ... Yang, Z. L. (2013). Technical description of version 4.5 of the Community Land Model (CLM). NCAR Technical Note NCAR/TN-503+STR. 420 pp, <https://doi.org/10.5065/d6rr1w7m>

Potter, C. S., Randerson, J. T., Field, C. B., Matson, P. A., Vitousek, P. M., Mooney, H. A., & Klooster, S. A. (1993). Terrestrial ecosystem production – a process model-based on global satellite and surface data. *Global Biogeochemical Cycles*, 7, 811– 841. <https://doi.org/10.1029/93gb02725>

Randerson, J. T., Thompson, M. V., Conway, T. J., Fung, I. Y., & Field, C. B. (1997). The contribution of terrestrial sources and sinks to trends in the seasonal cycle of atmospheric carbon dioxide. *Global Biogeochemical Cycles*, 11, 535– 560. <https://doi.org/10.1029/97GB02268>

Randerson, J. T., Thompson, M. V., Malmstrom, C. M., Field, C. B., & Fung, I. Y. (1996). Substrate limitations for heterotrophs: Implications for models that estimate the seasonal cycle of atmospheric CO₂. *Global Biogeochemical Cycles*, 10, 585– 602. <https://doi.org/10.1029/96GB01981>

Rasmussen, M., Hastings, A., Smith, M. J., Agosto, F. B., Chen-Charpentier, B. M., Hoffman, F. M., ... Luo, Y. (2016). Transit times and mean ages for nonautonomous and autonomous compartmental systems. *Journal of Mathematical Biology*, 73, 1379– 1398. <https://doi.org/10.1007/s00285-016-0990-8>

Schimel, J. (2001). 1.13 - Biogeochemical models: Implicit versus explicit microbiology. In E.-D. Schulze, M. Heimann, S. Harrison, E. Holland, J. Lloyd, I. C. Prentice & D. S. Schimel (Eds.), *Global biogeochemical cycles in the climate system* (pp. 177– 183). San Diego, IL: Academic Press.

Schimel, J. P., & Schaeffer, S. M. (2012). Microbial control over carbon cycling in soil. *Frontiers in Microbiology*, 3, 348. <https://doi.org/10.3389/fmicb.2012.00348>

Schmidt, M. W., Torn, M. S., Abiven, S., Dittmar, T., Guggenberger, G., Janssens, I. A., ... Nannipieri, P. (2011). Persistence of soil organic matter as an ecosystem property. *Nature*, 478, 49– 56. <https://doi.org/10.1038/nature10386>

Schuur, E. A., Vogel, J. G., Crummer, K. G., Lee, H., Sickman, J. O., & Osterkamp, T. E. (2009). The effect of permafrost thaw on old carbon

- release and net carbon exchange from tundra. *Nature*, 459, 556– 559. <https://doi.org/10.1038/nature08031>
- Sierra, C. A., Müller, M., & Trumbore, S. E. (2012). Models of soil organic matter decomposition: The SoilR package, version 1.0. *Geoscientific Model Development*, 5, 1045– 1060. <https://doi.org/10.5194/gmd-5-1045-2012>
- Sitch, S., Smith, B., Prentice, I. C., Arneeth, A., Bondeau, A., Cramer, W., ... Venevsky, S. (2003). Evaluation of ecosystem dynamics, plant geography and terrestrial carbon cycling in the LPJ dynamic global vegetation model. *Global Change Biology*, 9, 161– 185. <https://doi.org/10.1046/j.1365-2486.2003.00569.x>
- Sulman, B. N., Phillips, R. P., Oishi, A. C., Shevliakova, E., & Pacala, S. W. (2014). Microbe-driven turnover offsets mineral-mediated storage of soil carbon under elevated CO₂. *Nature Climate Change*, 4, 1099– 1102. <https://doi.org/10.1038/nclimate2436>
- Tian, H. Q., Lu, C. Q., Yang, J., Banger, K., Huntzinger, D. N., Schwalm, C. R., ... Huang, M. (2015). Global patterns and controls of soil organic carbon dynamics as simulated by multiple terrestrial biosphere models: Current status and future directions. *Global Biogeochemical Cycles*, 29, 775– 792. <https://doi.org/10.1002/2014gb005021>
- Todd-Brown, K. E. O., Randerson, J. T., Hopkins, F., Arora, V., Hajima, T., Jones, C., ... Zhang, Q. (2014). Changes in soil organic carbon storage predicted by earth system models during the 21st century. *Biogeosciences*, 11, 2341– 2356. <https://doi.org/10.5194/bg-11-2341-2014>
- Todd-Brown, K. E. O., Randerson, J. T., Post, W. M., Hoffman, F. M., Tarnocai, C., EaG, S., & Allison, S. D. (2013). Causes of variation in soil carbon predictions from CMIP5 earth system models and comparison with observations. *Biogeosciences*, 10, 1717– 1736. <https://doi.org/10.5194/bg-10-1717-2013>
- Wang, Y. P., Law, R. M., & Pak, B. (2010). A global model of carbon, nitrogen and phosphorus cycles for the terrestrial biosphere. *Biogeosciences*, 7, 2261– 2282. <https://doi.org/10.5194/bg-7-2261-2010>
- Wieder, W. R., Allison, S. D., Davidson, E. A., Georgiou, K., Hararuk, O., He, Y., ... Todd-Brown, K. (2015). Explicitly representing soil microbial processes in earth system models. *Global Biogeochemical Cycles*, 29, 1782– 1800. <https://doi.org/10.1002/2015gb005188>
- Wieder, W. R., Boehnert, J., Bonan, G. B., & Langseth, M. (2014). RegridDED harmonized world soil database v1.2. from Oak Ridge National Laboratory Distributed Active Archive Center, Oak Ridge, Tennessee, USA. Retrieved from <http://daac.ornl.gov/>, <https://doi.org/10.3334/ornlDaac/1247>

Wieder, W. R., Cleveland, C. C., Smith, W. K., & Todd-Brown, K. (2015). Future productivity and carbon storage limited by terrestrial nutrient availability. *Nature Geoscience*, 8, 441- 444. <https://doi.org/10.1038/ngeo2413>

Wieder, W. R., Grandy, A. S., Kallenbach, C. M., & Bonan, G. B. (2014). Integrating microbial physiology and physio-chemical principles in soils with the Mlcrobial-MIneral Carbon Stabilization (MIMICS) model. *Biogeosciences*, 11, 3899- 3917. <https://doi.org/10.5194/bg-11-3899-2014>

Wieder, W. R., Grandy, A. S., Kallenbach, C. M., Taylor, P. G., & Bonan, G. B. (2015). Representing life in the Earth system with soil microbial functional traits in the MIMICS model. *Geoscientific Model Development*, 8, 1789- 1808. <https://doi.org/10.5194/gmd-8-1789-2015>

Zhang, Q., Wang, Y. P., Matear, R. J., Pitman, A. J., & Dai, Y. J. (2014). Nitrogen and phosphorous limitations significantly reduce future allowable CO₂ emissions. *Geophysical Research Letters*, 41, 632- 637. <https://doi.org/10.1002/2013GL058352>

Zhao, M., Heinsch, F. A., Nemani, R. R., & Running, S. W. (2005). Improvements of the MODIS terrestrial gross and net primary production global data set. *Remote Sensing Of Environment*, 95, 164- 176. <https://doi.org/10.1016/j.rse.2004.12.011>